

Dielectric relaxation and polaronic hopping in the single-layered perovskite $\text{La}_{1.5}\text{Sr}_{0.5}\text{CoO}_4$ ceramics

W. Z. Yang · C. L. Song · X. Q. Liu ·
H. Y. Zhu · X. M. Chen

Received: 12 March 2011 / Accepted: 20 April 2011 / Published online: 3 May 2011
© Springer Science+Business Media, LLC 2011

Abstract Single tetragonal $\text{La}_{1.5}\text{Sr}_{0.5}\text{CoO}_4$ ceramics with the space group of $I\bar{4}/mm$ (139) were prepared by a solid-state reaction process, and dielectric characteristics were investigated on a broad frequency and temperature range. There was one obvious dielectric relaxation around room temperature plus a low temperature upturn on the curve of temperature dependence of dielectric properties for $\text{La}_{1.5}\text{Sr}_{0.5}\text{CoO}_4$ ceramics. This dielectric relaxation was a thermal-activated process. It should be attributed to the mixed-valence structure ($\text{Co}^{2+}/\text{Co}^{3+}$) since its activation energy was similar to that of small polaronic hopping process. After annealing the sample in O_2 atmosphere, dielectric constants and ac conductivities of $\text{La}_{1.5}\text{Sr}_{0.5}\text{CoO}_4$ ceramics increased and decreased after annealing the sample in N_2 atmosphere. This abnormal phenomenon should be attributed to the variation of concentration for holes (Co^{3+}).

Introduction

Cobaltates comprise a group of interesting materials which display spectacular properties such as giant magnetoresistance [1], superconductivity [2], large thermoelectric power [3], and ferro-ferri-antiferro-magnetic transitions with various forms of charge, orbital, and spin ordering [4–10]. A key aspect of cobaltates that distinguishes them from the manganates and cuprates is the spin state degree

of freedom of the Co^{3+} ions: it can be low spin (LS, $S = 0$), high spin (HS, $S = 2$), and even intermediate spin (IS, $S = 1$) [11].

Recently, the single-layered perovskite $\text{La}_{2-x}\text{Sr}_x\text{CoO}_4$ has received considerable attention for its extremely insulating behavior, peculiar magnetic correlations, and doping-dependent charge/spin superstructures, and its spin state issue becomes a vital topic [12–16]. Moritomo et al. [17] have observed significant reduction of resistivity with increasing x beyond ~ 0.7 , and concomitant reduction of the effective moment μ_{eff} from ≈ 4.0 to $\approx 2.6 \mu_B$. Judging from the magnitude of μ_{eff} , the spin-states of Co^{3+} and Co^{2+} ions are in the HS state for $x \leq 0.6$, while in the IS state for $0.8 \leq x \leq 1.0$, and the transition from the HS state to the IS state occurs for $0.6 \leq x \leq 0.8$.

Furthermore, $\text{La}_{1.5}\text{Sr}_{0.5}\text{CoO}_4$ compound, at half-doping in the $\text{La}_{2-x}\text{Sr}_x\text{CoO}_4$ system, exhibits an insulating charge-ordered and spin-ordered phase. Previous investigations have revealed a number of interesting features in the $\text{La}_{1.5}\text{Sr}_{0.5}\text{CoO}_4$. For instance, neutron scattering measurements of $\text{La}_{1.5}\text{Sr}_{0.5}\text{CoO}_4$ by Zaliznyak et al. show a checkerboard $\text{Co}^{2+}-\text{Co}^{3+}$ charge order and a strongly decreasing spin ordering temperature ($T_{\text{SO}} \approx 30$ K), and they suggest the Co^{3+} ions to be in an IS but nonmagnetic state quenched by strong planar anisotropy at low temperature. At higher temperature, a spin-entropy driven transition to the HS state occurs with consequent disappearance of the Jahn–Teller modulation and conspicuous melting of the charge order [18, 19]. A very recent X-ray absorption spectroscopic study by Chang et al. [11] establishes a picture of HS Co^{2+} and LS Co^{3+} for $\text{La}_{1.5}\text{Sr}_{0.5}\text{CoO}_4$, and their study well accounts for the extremely insulating nature of the $\text{La}_{2-x}\text{Sr}_x\text{CoO}_4$ series, the high charge-ordering temperature ($T_{\text{CO}} \approx 750$ K) and low spin ordering temperature (T_{SO}) of $\text{La}_{1.5}\text{Sr}_{0.5}\text{CoO}_4$.

W. Z. Yang · C. L. Song · X. Q. Liu (✉) ·

H. Y. Zhu · X. M. Chen

Laboratory of Dielectric Materials, Department of Materials Science and Engineering, Zhejiang University, Hangzhou 310027, China
e-mail: xqliu@zju.edu.cn

On the other hand, the observation of giant dielectric constant materials has aroused tremendous interest for potential technological applications since the discovery of the $\text{CaCu}_3\text{Ti}_4\text{O}_{12}$ [20]. Recently, the giant dielectric responses up to high frequency are found in the K_2NiF_4 -type $\text{Ln}_{2-x}\text{Sr}_x\text{NiO}_4$ ceramics [21–24]. For example, Krohns et al. [23] have observed an extremely high dielectric constant in $\text{La}_{15/8}\text{Sr}_{1/8}\text{NiO}_4$ up to gigahertz at room temperature; the reason is proposed to be the charge ordering(CO)-induced heterogeneity, and which arises on a much finer scale than grain boundary. If the CO is really related to giant dielectric response, other materials with a certain kind of charge-ordered state should also exhibit a giant dielectric constant. This may open up a new research opportunity since one could explore this mechanism clearly in the materials design. So, it is worth to investigate the dielectric properties of $\text{La}_{1.5}\text{Sr}_{0.5}\text{CoO}_4$ materials because it is a typical charge-ordered phase in a wide temperature range. However, the dielectric properties of $\text{La}_{1.5}\text{Sr}_{0.5}\text{CoO}_4$ materials are rarely reported to our knowledge.

In this study, we focus on the dielectric properties of $\text{La}_{1.5}\text{Sr}_{0.5}\text{CoO}_4$ ceramics in a broad frequency and temperature range, with the aim of investigating the relationship between dielectric response and CO. The correlation between the dielectric response and spin ordering should be studied in the future because of its low spin ordering temperature.

Experimental conditions

The $\text{La}_{1.5}\text{Sr}_{0.5}\text{CoO}_4$ powders were synthesized by a solid-state reaction process using the starting materials of La_2O_3 (99.99%), Co_2O_3 (99%), and SrCO_3 (99.9%), which were weighed and mixed by ball milling with ZrO_2 balls in ethanol for 24 h, then dried and calcined at 1150 °C in air for 3 h to yield the desired materials. The calcined powders were ball milled for 24 h and then dried. The calcined powders with 7 wt% polyvinyl alcohol (PVA) were pressed into pellets and then sintered in air at 1350 °C for 3 h. The relative density for $\text{La}_{1.5}\text{Sr}_{0.5}\text{CoO}_4$ ceramics is 95% of the theoretic density. Some $\text{La}_{1.5}\text{Sr}_{0.5}\text{CoO}_4$ samples were annealed at 1150 °C for 6 h in a flow of O_2 or N_2 to understand the origin of dielectric relaxation. The crystalline phase was identified by powder X-ray diffraction using Cu K_α radiation (Rigaku D/max 2550 PC, Rigaku Co., Tokyo, Japan). The dielectric characteristics and ac conductivities of these ceramics were evaluated with a broadband dielectric spectrometer (Turnkey Concept 50, Novocontrol Technologies GmbH & Co., Hundsangen, Germany) in a broad range of temperature (133–450 K) and frequency (2 kHz–1 MHz) with a heating rate of 2 K/min, and the silver paste was adopted as electrodes.

Results and discussion

Figure 1 shows the XRD pattern of the $\text{La}_{1.5}\text{Sr}_{0.5}\text{CoO}_4$ ceramics sintered at 1350 °C for 3 h. Single tetragonal $\text{La}_{1.5}\text{Sr}_{0.5}\text{CoO}_4$ ceramics with the space group $I\ 4/mmm$ (139) are obtained, and there is no trace of impurities as shown in the XRD pattern.

The temperature dependence of dielectric properties for $\text{La}_{1.5}\text{Sr}_{0.5}\text{CoO}_4$ ceramics at different frequencies (2 kHz–1 MHz) is shown in Fig. 2. One obvious dielectric relaxation around room temperature is observed, which shows strong frequency dispersion. Besides this obvious relaxation, a small upturn is observed below the relaxation. The upturn is so small that there is almost no evidence on the curve of the temperature dependence of dielectric loss, so we just focus on the dielectric relaxation around room temperature. The dielectric constant (ϵ') slowly increases with increasing temperature first, and then a significant increase is observed at a critical temperature. The critical temperatures for dielectric relaxation increase with increasing frequency. As shown in Fig. 2b, a dielectric loss ($\tan\delta$) peak corresponding to the dielectric relaxation shifts to higher temperature with increasing frequency, indicating a thermally activated process. To analyze this dielectric relaxation, the frequency dependence of peak temperature for the dielectric loss is plotted, and the following relationship is involved,

$$f = f_0 \exp\left(-\frac{Q}{k_B T_m}\right), \quad (1)$$

where Q denotes the activation energy required for the dielectric relaxation, k_B is Boltzmann's constant, f is the applied frequency, f_0 is the pre-exponential factor, and T_m is the temperature where the dielectric loss is maximum. The T_m values are directly obtained from the experimental

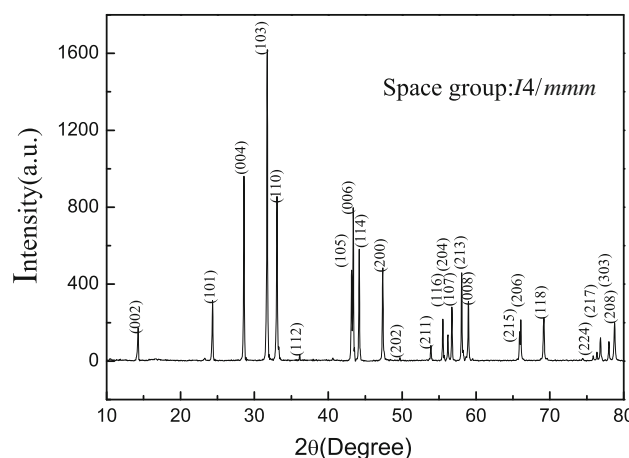


Fig. 1 X-ray powder diffraction pattern of $\text{La}_{1.5}\text{Sr}_{0.5}\text{CoO}_4$ ceramics at room temperature

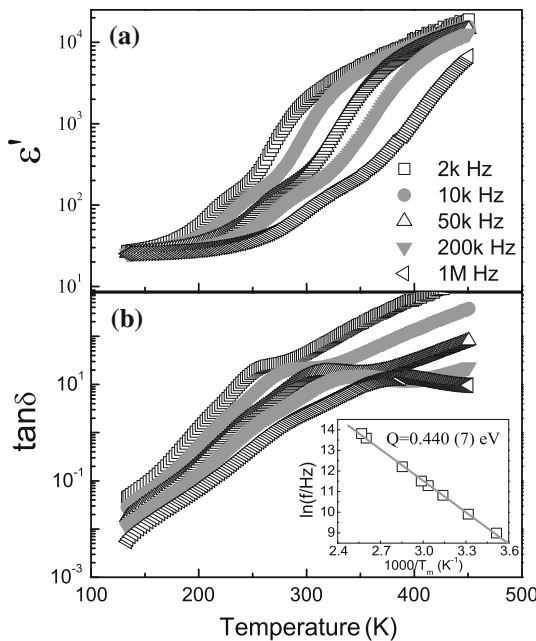


Fig. 2 Temperature dependence of dielectric properties of $\text{La}_{1.5}\text{Sr}_{0.5}\text{CoO}_4$ ceramics: **a** dielectric constant and **b** dielectric loss. The inset shows the Arrhenius fitting for dielectric relaxation of $\text{La}_{1.5}\text{Sr}_{0.5}\text{CoO}_4$ ceramics

data instead of curve fitting. That is, we recognize the temperature where the measured dielectric loss is highest in the vicinity of dielectric relaxation as the T_m although the value determined from this method is sometime inexact. After fitting the data at various frequencies (8, 20, 50, 80, 100, 200, 800 kHz, and 1 MHz) with Eq. 1, the following results are obtained: the activation energy is 0.440 ± 0.007 eV (see the inset of Fig. 2).

The frequency-dependent conductivity $\sigma(f)$ as shown in Fig. 3a is characterized in the temperature range of 186–400 K. The $\sigma(f)$ decreases first and then it almost keep a constant value at low frequencies. The bulk conductivity follows an universal dielectric response behavior governed by the equation [25]

$$\sigma = \sigma_{dc} + A\omega^n, \quad (2)$$

where σ_{dc} is the bulk dc conductivity, A and n are temperature-dependent constants. Good agreement between experimental and fitting data is achieved. The electrical transport behavior of $\text{La}_{1.5}\text{Sr}_{0.5}\text{CoO}_4$ ceramics has been found to follow small polaronic hopping mechanism at the whole temperature [26, 27],

$$\sigma_{dc}T = \sigma_0 \exp(-E_a/k_B T), \quad (3)$$

where σ_0 is pre-exponential factor proportional to the density of charge carries, E_a the activation energy required for polaronic conduction. The temperature dependence of σ_{dc} , along with the fitting result is shown in Fig. 3b. It shows the $\text{La}_{1.5}\text{Sr}_{0.5}\text{CoO}_4$ ceramics have two thermally

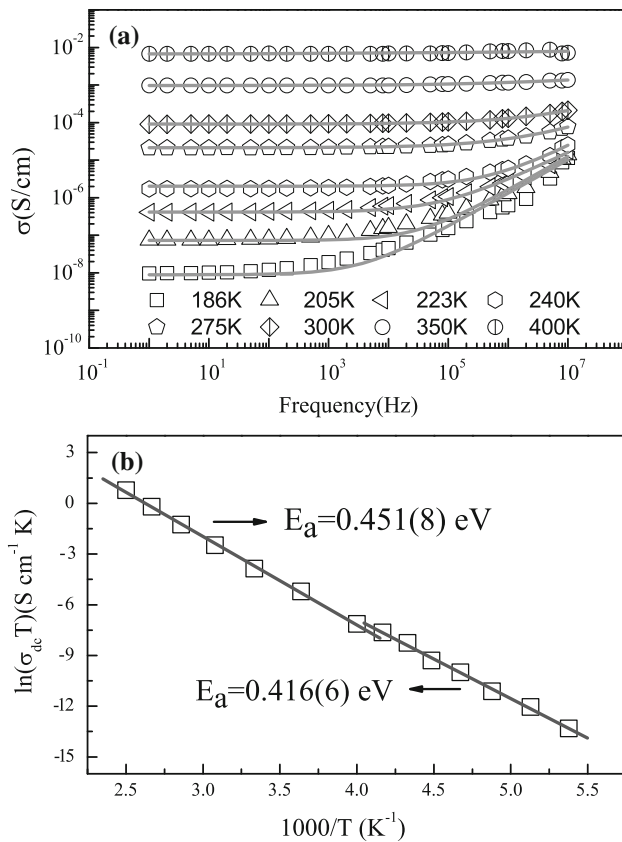


Fig. 3 **a** Frequency dependence of ac conductivity for $\text{La}_{1.5}\text{Sr}_{0.5}\text{CoO}_4$ ceramics at relaxation temperatures. The solid lines are fitting results according to universal dielectric response behavior. **b** Temperature dependence of dc conductivity for $\text{La}_{1.5}\text{Sr}_{0.5}\text{CoO}_4$ ceramics. The solid line is fitting results according to polaronic theory

activated conduction processes. The small polaron hopping activation energy E_a is 0.451 ± 0.008 eV at the relaxation temperature (250–400 K). The dielectric relaxation activation energy is close to that of small polaronic hopping process. Therefore, the dielectric relaxation of $\text{La}_{1.5}\text{Sr}_{0.5}\text{CoO}_4$ ceramics may originate from the Co^{2+} – Co^{3+} mixed-valence structure, i.e., dipolar effect associates with localized charge carriers (polarons) hopping between spatially fluctuating lattice potentials. In $\text{La}_{1.5}\text{Sr}_{0.5}\text{CoO}_4$ ceramics, the existence of Co^{2+} and Co^{3+} is revealed by a lot of experiments and calculations [11, 18, 19]. Similar to nickelates and manganites, the main charge carrier is the holes located at Co^{3+} ions. They may walk around in the form of small polarons under applied electric field because they are bound to Co^{3+} ions. Therefore, the intersite hopping of polarons under ac electric field contributes to dielectric relaxation, while the transport of polarons through Co^{2+} – O – Co^{3+} linked path under dc electric field produce dc conduction [28, 29]. On the other hand, the small polaron hopping activation energy E_a is 0.416 ± 0.006 eV at lower temperature (186–240 K). This value is much different from the small polaron hopping activation energy ($E_a = 0.451 \pm 0.008$ eV) at the

relaxation temperature (250–400 K). It looks like there may be two different polarization mechanisms. Meanwhile, the low temperature dielectric constant is rather low compared with the high temperature dielectric constant. This phenomenon may attribute to the different polarization mechanism.

In order to get more clarifying information about the mechanisms of the dielectric relaxation, identical annealing treatments first in O₂ and second in N₂ are performed on La_{1.5}Sr_{0.5}CoO₄ ceramics. After each treatment, dielectric properties are measured as a function of temperature. Figure 4 presents dielectric constants and dielectric losses of as-sintered (solid), N₂-annealed (triangular), O₂-annealed (circle) La_{1.5}Sr_{0.5}CoO₄ ceramics at the frequency of 1 MHz. The inset shows the comparison of ac electrical conductivities of as-sintered, N₂-, and O₂-annealed samples at room temperature. It is clearly seen that oxygen annealing significantly enhances dielectric constants and dielectric losses, and the ac conductivities of O₂-annealed sample are larger than those of the as-sintered one at room temperature. However, both the dielectric constants and ac conductivities are strongly suppressed after the nitrogen annealing. The values of dielectric constants and ac conductivities are almost same as those of as-sintered sample. While in the common oxide ceramics, the electrical conductivities of ceramics will increase after the nitrogen annealing, while

they decrease after the oxygen annealing, since some oxygen vacancies have been created during the sintering process. This anomaly phenomenon should be attributed to the changes in the concentration of holes (Co³⁺). The holes (Co³⁺) concentration increases after annealing the sample in oxygen atmosphere due to the capability of K₂NiF₄-type arrangements for accommodating extra oxygen in the interstitials of the structure [30], so charge carriers transport more easily than those in as-sintered sample. Therefore, the ac conductivities of O₂-annealed sample are larger than those of the as-sintered sample. Meanwhile, the dielectric constants and dielectric loss are closely related with the holes concentration. With increasing the holes (Co³⁺) concentration, the small polarons concentration also enhances [26]. So, dielectric constants and dielectric losses greatly increased after annealing in oxygen atmosphere. However, nitrogen can create a reduction-like atmosphere. The holes (Co³⁺) concentration decreases and small polaron concentration is reduced by annealing the sample in nitrogen atmosphere. This will remove the effect of O₂ annealed. Therefore, dielectric constants and ac conductivities of La_{1.5}Sr_{0.5}CoO₄ ceramics are almost same as those of as-sintered sample after annealing in nitrogen atmosphere. It looks like there may be two different polarization mechanisms. Meanwhile, the low temperature dielectric constant is rather compared low with the high-temperature dielectric constant. This phenomenon may attribute to the different polarization mechanism.

Conclusion

In summary, high dielectric response has been found in the single-layered perovskite La_{1.5}Sr_{0.5}CoO₄ ceramics. There was one obvious dielectric relaxation around room temperature plus a low temperature upturn on the curve of temperature dependence of dielectric properties of La_{1.5}Sr_{0.5}CoO₄ ceramics. The dielectric relaxation was a thermal-activated process. It should be attributed to the mixed-valence structure (Co²⁺/Co³⁺) since the activation energy was similar to that of small polaronic hopping process. After annealing the sample in O₂ atmosphere, the dielectric permittivity and ac conductivities of La_{1.5}Sr_{0.5}CoO₄ ceramics increased, and they decreased after annealing the sample in N₂ atmosphere. This abnormal phenomenon should be attributed to the variation of concentration for holes (Co³⁺). So, we confirm the relationship between high dielectric response and charge inhomogeneous in the single-layered perovskite La_{1.5}Sr_{0.5}CoO₄ ceramics.

Acknowledgements This study was supported by National Science Foundation of China under Grant Nos. 50832005 and 50702049, Chinese National Key Project for Fundamental Researches under Grant No. 2009CB623302, and the Fundamental Research Funds for Central Universities under Grand No. 2010QNA4006.

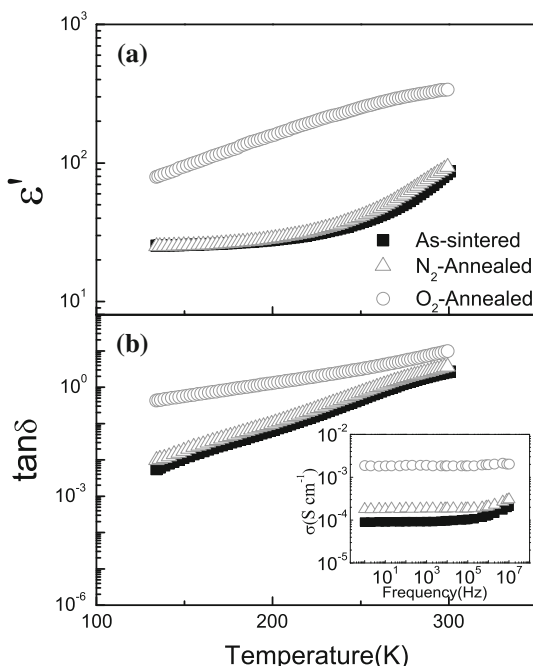


Fig. 4 **a** Dielectric constants and **b** dielectric losses of as-sintered (filled square), O₂-annealed (open circle), N₂-annealed (open triangle) La_{1.5}Sr_{0.5}CoO₄ ceramics at the frequencies of 1 MHz. The inset shows the comparison of ac electrical conductivities of as-sintered (filled square), O₂-annealed (open circle), and N₂-annealed (open triangle) samples at room temperature

References

1. Troyanchuk IO, Kasper NV, Khalyavin DD, Szymczak H, Szymczak R, Baran M (1998) Phys Rev Lett 80:3380
2. Takada K, Sakurai H, Takayama-Muromachi E, Izumi F, Dilanian RA, Sasaki T (2003) Nature (London) 422:53
3. Terasaki I, Sasago Y, Uchinokura K (1997) Phys Rev B 56:R12685
4. Vogt T, Woodward PM, Karen P, Hunter BA, Henning P, Moodenbaugh AR (2000) Phys Rev Lett 84:2969
5. Niitaka S, Yoshimura K, Kosuge K, Nishi M, Kakurai K (2001) Phys Rev Lett 87:177202
6. Taskin AA, Lavrov AN, Ando Y (2003) Phys Rev Lett 90:227201
7. Kudasov YB (2006) Phys Rev Lett 96:027212
8. Cwik M, Benomar M, Finger T, Sidis Y, Senff D, Reuther M, Lorenz T, Braden M (2009) Phys Rev Lett 102:057201
9. Boothroyd AT, Babkevich P, Prabhakaran D, Freeman PG (2011) Nature (London) 471:341
10. Helme LM, Boothroyd AT, Coldea R, Prabhakaran D, Frose CD, Keen DA, Regnault LP, Freeman PG, Enderle M, Kulda J (2009) Phys Rev B 80:134414
11. Chang CF, Hu Z, Wu H, Burnus T, Hollmann N, Benomar M, Lorenz T, Tanaka A, Lin HJ, Hsieh HH, Chen CT, Tjeng LH (2009) Phys Rev Lett 102:116401
12. Wu H, Burnus T (2009) Phys Rev B 80:081105(R)
13. Shimada Y, Miyasaka S, Kumai R, Tokura Y (2006) Phys Rev B 73:134424
14. Chichev AV, Dlouhá M, Vratislav S, Knížek K, Hejtmánek J, Maryško M, Veveřka M, Jirák Z, Golosova NO, Kozlenko DP, Savenko BN (2006) Phys Rev B 74:134414
15. Savici AT, Zaliznyak IA, Gu GD, Erwin R (2007) Phys Rev B 75:184443
16. Sakiyama N, Zaliznyak IA, Lee SH, Mitsui Y, Yoshizawa H (2008) Phys Rev B 78:180406(R)
17. Moritomo Y, Higashi K, Matsuda K, Nakamura A (1997) Phys Rev B 55:R14725
18. Zaliznyak IA, Hill JP, Tranquada JM, Erwin R, Moritomo Y (2000) Phys Rev Lett 85:4353
19. Zaliznyak IA, Tranquada JM, Erwin R, Moritomo Y (2001) Phys Rev B 64:195117
20. Homes CC, Vogt T, Shapiro SM, Wakimoto S, Ramirez AP (2001) Science 293:673
21. Liu XQ, Wu SY, Chen XM, Zhu HY (2008) J Appl Phys 104:054114
22. Liu XQ, Wu YJ, Chen XM, Zhu HY (2009) J Appl Phys 105:054104
23. Krohns S, Lunkenheimer P, Kant Ch, Pronin AV, Brom HB, Nugroho AA, Diantoro M, Loidl A (2009) Appl Phys Lett 94:122903
24. Lunkenheimer P, Krohns S, Riegg S, Ebbinghaus SG, Reller A, Loidl A (2010) Eur Phys J Special Top 180:61
25. Preethi Meher KRS, Varma KBR (2009) J Appl Phys 105:034113
26. Iguchi E, Nakatsugawa H, Futakuchi K (1998) J Solid State Chem 139:176
27. Liu XQ, Yang WZ, Song CL, Chen XM (2010) Appl Phys A 100:1131
28. Jaime M, Hardner HT, Salamon MB, Rubinstein M, Dorsey P, Emin D (1997) Phys Rev Lett 78:951
29. Lin YQ, Chen XM (2010) Appl Phys Lett 96:142902
30. Song CL, Wu YJ, Liu XQ, Chen XM (2010) J Alloys Compd 490:605